Received: 24 October 2021 | Revised: 4 February 2022 | Accepted: 8 February 2022

DOI: 10.1002/tqem.21862

RESEARCH ARTICLE

WILEY

Impact of COVID-19 lockdown on the elemental profile of PM_{10} present in the ambient aerosol of an educational institute in Kolkata, India

Praveen Tudu[1] | **Tanushree Gaine**[1,2] | **Shouvik Mahanty**[1] | **Sayantani Mitra**[1] | **Subarna Bhattacharyya**[3] | **Punarbasu Chaudhuri**[1]

[1]Department of Environmental Science, University of Calcutta, Kolkata, West Bengal, India

[2]Department of Environmental Studies, New Alipore College, Kolkata, West Bengal, India

[3]School of Environmental Studies, Jadavpur University, Kolkata, West Bengal, India

Correspondence
Punarbasu Chaudhuri, Department of Environmental Science, University of Calcutta, Kolkata, West Bengal 700019, India.
Email: punarbasu_c@yahoo.com

Abstract

Reduction in air pollution level was prime observation during COVID-19 lockdown globally. Here, the study was conducted to assess the impact of lockdown on the elemental profile of PM_{10} in ambient aerosol to quantify the elemental variation. To quantify the variation, phase-wise sampling of air pollutants was carried out using the gravimetric method for PM_{10}, while NO_2 and SO_2 were estimated through the chemiluminescence and fluorescent spectrometric method respectively. The elemental constituents of PM_{10} were carried out using an Inductively Coupled Plasma Optical Emission Spectrometer and their source apportionment was carried out using the Positive Matrix Factorization model. The results showed that PM_{10}, NO_2 and SO_2 reduced by 86.97%, 83.38%, and 88.60% respectively during the lockdown sampling phase. The highest mean elemental concentration reduction was found in Mn (97.47%) during the lockdown. The inter-correlation among the pollutants exhibited a significant association indicating that they originate from the same source. The metals like Mn and Cu were found at a higher concentration during the lockdown phase corresponding to vehicular emissions. The comparative analysis of the elemental profile of PM_{10} concluded that the lockdown effectuated in reduction of the majority of elements present in an aerosol enveloping metropolitan like Kolkata.

KEYWORDS
air quality, COVID-19 lockdown, particulate matter, source apportionment, urban emissions

1 | INTRODUCTION

Kolkata, which has been one of the fast-growing cities in India, harbors more than 14.5 million people including the suburb (Dutta et al., 2021), which presents various challenges in regards to waste management and pollution control. Various sources of heavy metal have been identified in and around Kolkata like metal industries, tanneries (Karar et al., 2006), and powerplants (Diong et al., 2016). The study by Gupta et al. (2007) has estimated that the contribution of coal combustion to PM_{10} and total suspended particulate (TSP) matter accounts for 34% and 17%, respectively, in the industrial sites whereas the residential sites contribute around 42% and 37%, respectively.

Apart from heavy traffic load and industrial emission, ambient air quality in Kolkata is heavily influenced by the constant construction activities within the Kolkata metropolitan area (Barman et al., 2009). The city also comes under heavy stress during festive seasons like Diwali where metal concentrations were found to be 70–80 times higher for Cobalt (Co) and Vanadium (V) compared to normal days and 25–40 times higher for Copper (Cu), Iron (Fe) and Manganese (Mn) when compared to normal days, whereas the water-soluble ionic

components were found to be approximately 1.5–6 times higher (Chatterjee et al., 2013). A study by Gajghate et al. (2005) shows that the aerosol metal profile of Kolkata exhibited elements like Lead (Pb), Cadmium (Cd), Nickel (Ni), Zinc (Zn), Aluminum (Al) and Iron (Fe), predominantly present at residential and industrial sites.

These heavy metal concentrations in the aerosol are major factors responsible for various health complications like cardiovascular diseases (Chen et al., 2005; Dockery et al., 2005), heavy metal poisoning, asthma (Liu et al., 2017), bronchitis (Barnett et al., 2005) and complication during pregnancy and birth defects (Liu et al., 2003). These complications are extensively studied around the globe emphasizing the adverse effect on human health. The study by Sangani et al. (2010) shows that heavy metals even at nanogram (ng) level are potent enough to diminish blood coagulation time, while Becker and Soukup (2003) found that air pollutants are responsible for a surge in costimulatory molecules in the human immune system.

These metals which are also major constituents of particulate matter have been a major concern for every governing body to improve the air quality under their jurisdiction. Coincidentally COVID-19 pandemic was one such moment in recent times where restrictions over most of the anthropogenic activities paved the much-needed air pollution assessment in identifying the areas which need the right implementation of solutions for minimizing the emission of pollutants (Mahato et al., 2020; Sarkar et al., 2021). The abrupt restriction of anthropogenic activities was implemented in India from March 24, 2020 (Kabiraj & Gavli, 2020; Srivastava et al., 2020), constraining the normal movement of the population (Gautam & Hens, 2020). Like the whole country, interstate and intrastate transportation from Kolkata were suspended till May 3, 2020, which was further extended till June 30, 2020 in areas with large COVID-19 cases categorized as red zones (Banerji & Mitra, 2021; Nath et al., 2021). During the lockdown, the Indian railway was operating only freight services to transport necessary goods to various parts of the country. The intracity goods carriers in Kolkata were permitted to supply necessary goods to every corner of the city. The government centers, banks and food processing industries were permitted to operate from June 8, 2020 with a 50% workforce and implementing necessary social distancing norms (Banerji & Mitra, 2021). The relaxation on interstate transportation, shopping malls and religious gathering was granted in areas with a negligible number of cases categorized as a green zone. The weekly assessment of COVID-19 cases was conducted to designate the red zones which continued till November 2020. The implementation of curfews and restrictions during lockdown was well studied to assess its impact on the environment (Sarkar et al., 2021), economy and health (Banerji & Mitra, 2021). The COVID-19 lockdown improved the quality of the ambient air around the globe signifying the effect of regulated restrictions on anthropogenic activities and their impact on human health (Banerji & Mitra, 2021). Ballygunge, an industrial locality of Kolkata experienced a reduction in pollutant concentration by approximately six times during lockdown in comparison to the pre-lockdown phase as quantified by Sarkar et al. (2021) in their study, where they observed that despite a reduction in pollutant concentration, Ballygunge suffered from pollutant load from Garden Reach and small-scale industries located nearby. These studies on COVID-19 lockdown on Kolkata and the rest of the world are based on either data acquired through automatic stations (Dutta et al., 2021; Sarkar et al., 2021) or from the satellite (Muhammad et al., 2020), which provides the variation in pollution load but fails to exhibit the proportion of elemental variation. Therefore, the purpose of this study was to quantify the impact of lockdown on air pollutants like PM_{10}, NO_2, SO_2 and elemental profile (Cr, Al, Zn, Fe, Mn, Co, Cu, Pb, Ni and Cd) of the ambient aerosol in Kolkata during the lockdown.

The intracity goods carriers in Kolkata were permitted to supply necessary goods to every corner of the city

2 | METHODOLOGY

2.1 | Sampling site

The aerosol sampling was carried out in the University of Calcutta's Taraknath Palit Siksha Prangan campus (22.526 N 88.363 E) as illustrated in **Exhibit 1**, which is situated in Ballygunge, an urban locality in the central part of Kolkata. The sampling site is surrounded by clusters of small-scale industrial units mainly comprised of tanneries and metal processing units as described by Kabiraj and Gavli (2020) in their study. They also mentioned the major pollutant contributors as traffic, industrial units and power plants, which was further elaborated in a study by Sarkar et al. (2021). The sampling site's close proximation to various small-scale industries, tanneries and road junctions favored the establishment of various pollutant sources through aerosol sampling.

2.2 | Sampling schedule

The sampling of ambient air quality was carried out thrice a month with a gap between two consecutive sampling days in four phases in the following manner:

Normal sampling (NS) phase: October 04–28, 2019 (NS1), November 04–24, 2019 (NS2) and December 04–24, 2019 (N3).

Pre-lockdown (PL) phase: January 04–24, 2020 (PL1), February 04–24, 2020 (PL2) and March 04–24, 2020 (PL3).

Lockdown (LD) phase: June 04–24, 2020.

Post-lockdown (PT) phase: September 04–24, 2020 (PT1), October 04–24, 2020 (PT2) and November 04–24, 2020 (PT3).

The respirable dust sampler (RDS) (Envirotech APM 460NL) and gaseous pollutant sampler (Envirotech APM 433) were used for the collection of particulate matter (PM_{10}), gaseous pollutants (NO_2 and SO_2) respectively from the ambient aerosol. The duration of

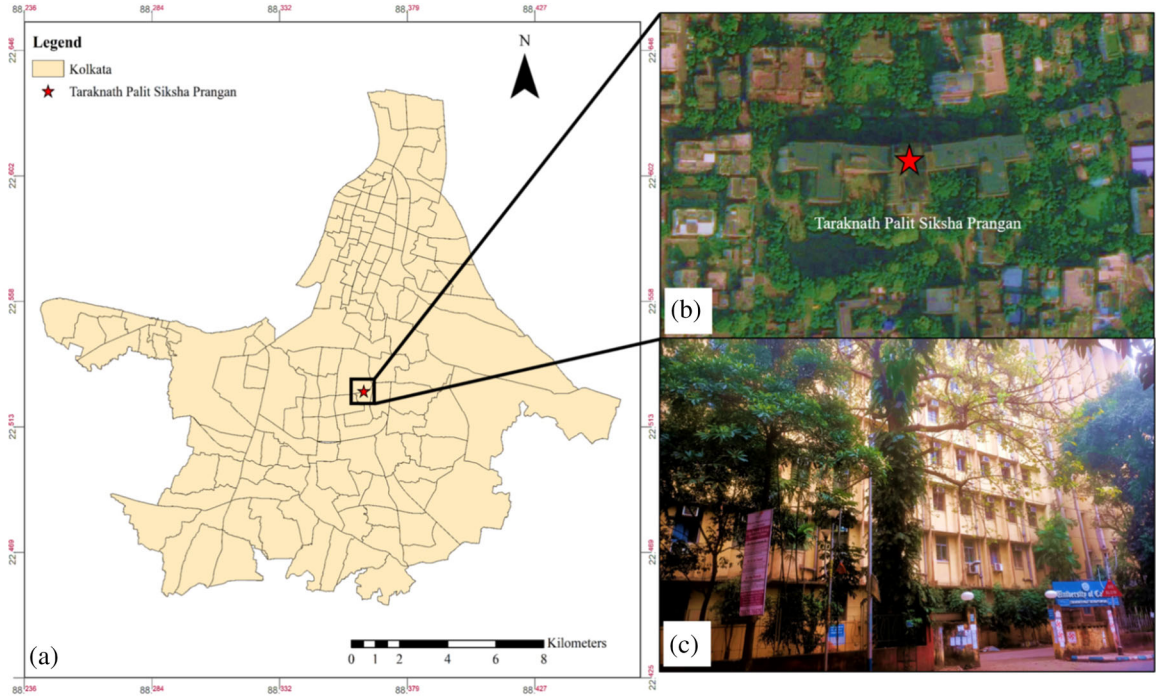

EXHIBIT 1 Figure illustrating: (a) Kolkata Municipal Corporation, (b) top view of sampling site and (c) street view of the sampling site [Color figure can be viewed at wileyonlinelibrary.com]

particulate sampling was carried out for 8 h (daytime: 10:00 a.m.–6:00 p.m.) while gaseous sampling was carried out for 6 h (daytime: 10:00 a.m.–4:00 p.m.) each. The samplers were placed within 3–10 m from the ground level, 20 m away from nearby trees and at a suitable distance from the direct pollution source.

2.3 | Lockdown timeline

The LD phase sampling was conducted in June 2020 when limited intracity traffic was allowed, while from March 24, 2020 to May 3, 2020 was complete lockdown as mentioned by Gautam and Hens (2020), which was extended till June 30, 2020 with restriction concentrated in red zones (Banerji & Mitra, 2021).

2.4 | Monitoring and analysis

The PM_{10} was collected on a pre-desiccated and pre-weighted glass microfiber filter (Micro separation) using RDS at an operating flow rate of approximately 1.2 m^3 min^{-1} for 8 h on each sampling day. The concentration of the particulate was computed by calculating the net mass difference over the total volume of air sampled. Gaseous pollutants (SO_2 and NO_2) from the ambient air were collected by allowing the air to pass through impingers for 6 h at the flow rate of 1–2 L min^{-1}.

SO_2 absorbing solution of 0.04 M potassium tetrachloromercurate (TCM) (10.86 g mercuric chloride, 0.066 g ethylenediaminetetraacetic acid (EDTA) and 6.0 g potassium chloride in 1000 mL H_2O) and NO_2 absorbing solution (4.0 g of sodium hydroxide and 1.0 g of sodium arsenite diluted to 1000 mL with distilled water) were filled into impinger at the beginning of sampling. The analysis of the SO_2 absorbing solution was carried out following the fluorescent spectrometric method using pararosaniline and methylsulphamic acid, whereas NO_2 absorbing solution was analyzed by chemiluminescence method using sulphanilamide, phosphoric acid and N(1-naphthyl) ethylenediamine dihydrochloride as described in guidelines for quantification of ambient air pollutants by CPCB (2013). The absorbance of the SO_2 solution was measured at 560 nm while NO_2 was determined at 540 nm (Lodge, 1988). The limit of detection (LOD) and limit of quantification (LOQ) of gaseous pollutant monitoring was calculated using the following formulas (Equations 1 and 2) from the study by Villanueva et al. (2021):

$$LOD = \frac{3\ x\ SD}{b} \quad (1)$$

$$LOQ = \frac{10\ x\ SD}{b} \quad (2)$$

where, SD: standard deviation of blank; and b: the slope of the linear regression between standard deviation and absorbance.

2.5 | Analysis of metals

The analysis for metals (Cu, Cr, Al, Zn, Fe, Mn, Co, Pb, Ni and Cd) was carried out using PM_{10} filter papers by modifying the prescribed method by Zalakeviciute et al. (2020), as described in the following

section. The elemental profile of the aerosol was divided into two categories:

a. major metals (> 10,000 ngm^{-3})- Al and Fe.
b. trace metals (< 100 ngm^{-3})- Cr, Zn, Cu, Ni, Pb, Co, Cd, and Mn.

Approximately 0.05 g of the circular disc was punched out from sample and blank filter paper, which were then digested using 10 mL of 65% HNO_3 in a microwave digester. The digestion program was set as follows:

Step 1- ramping the temperature to 110°C for 20 min on 1200 W followed by dwelling time of 5 min.
Step 2- ramping the temperature to 170°C for 15 min on 1200 W followed by dwelling time of 2.5 min, then further ramping the temperature to 185°C for 3 min on 1200 W followed by dwelling time of 10 min.

The digested samples were then left for cooling at room temperature and then the content was diluted to 50 mL using Milli-Q water. After that the digested samples were filtered using a syringe filter to eliminate any suspended particles. Each filtrate was then analyzed in inductively coupled plasma optical emission spectroscopy (ICP-OES) (Thermo Scientific iCAP-7000) along with the blank filtrate. To attend the analytical accuracy the experiment was conducted along with standard reference material of estuarine sediment standard reference material (SRM) 1646a acquired from the National Institute of Standards and Technology (NIST) and the percentage recovery was estimated between 92 and 110% and precision less than 5% of relative standard deviation for all metals and details are incorporated in the supplementary file (Table ST1).

2.6 | Meteorological data analysis

Meteorological parameters like average temperature (at), relative humidity (rh), barometric pressure (bp), wind speed (ws) and wind direction (wd) for the sampling phase were downloaded from Central Pollution Control Board (CPCB, https://app.cpcbccr.com) which has an automatic air pollution monitoring station situated in Ballygunge, approximately one km from the sampling site. Collected data was used in the assessment of the seasonal variation of pollutants and for the identification of local pollution sources. The seasonal variation in meteorological parameters during the entire sampling phase has been illustrated in Figure SF1.

Back-trajectory analysis for long-range air parcels was carried out using Hybrid Single-Particle Lagrangian Integrated Trajectory (HYSPLIT, https://www.ready.noaa.gov/HYSPLIT.php) to find the possible paths of air mass transportation which may have influenced the pollution concentration of local source contributors (Guo et al., 2009; Khobragade & Ahirwar, 2019). The 72 h backward trajectories were considered for each sampling day computing the arrival of air parcels at the interval of 6 h (6:00, 12:00, 18:00, and 00:00 (consecutive day) UTC) at the sampling site following the method described by Bodor et al. (2020) with slight modifications in arrival heights of 500, 1000, and 1500 m above ground level (agl) to accommodate the layers due to thermal inversions created by the Bay of Bengal as mentioned in a study by Deka et al. (2016).

2.7 | Statistical analysis

The pollutant and elemental concentrations were $\log_{10}$ transformed to have a homogenous approach. The transformed data were assessed for normal distribution using a quantile-quantile (Q-Q) plot as represented in Figure SF2, while two-way analysis of variance (ANOVA) and Dunnett's multiple comparisons test was carried out in IBM SPSS Statistics (version 25) for their significance among the pollutant means as shown in **Exhibits 2** and **3**.

The two-way ANOVA was carried out based on the formula by Pandis (2016):

$$SS_{TOTAL} = SS_A + SS_B + SS_{AB} + SS_E \tag{3}$$

where, SS_{TOTAL} : total variance between factors; SS_A : variance in factor A; SS_B : variance in factor B; SS_{AB} : variation due to interaction between factor A and B; and SS_E : random variation.

When,

$$SS_A = cn' \sum_{i=1}^{r} \left(\overline{X_i} - \overline{\overline{X}}\right)^2 \tag{4}$$

$$SS_B = rn' \sum_{j=1}^{c} \left(\bar{X}_j - \overline{\overline{X}}\right)^2 \tag{5}$$

$$SS_{AB} = n' \sum_{i=1}^{r} \sum_{j=1}^{c} \left(\overline{X_i} - \overline{\overline{X}}\right) - \left(\bar{X}_j - \overline{\overline{X}}\right)^2 \tag{6}$$

$$SS_E = \sum_{i=1}^{r} \sum_{j=1}^{c} \sum_{k=1}^{n'} \left(X_{ijk} - \bar{X}_{ij}\right)^2 \tag{7}$$

where c : number of levels of factor B (sampling phase); n' : number of replications for each cell; r : number of levels of factor A (pollutants and elements); X_{ijk} : the value of the k^{th} observation of level I of factor A and level j of factor B; $\overline{\overline{X}}$: grand mean; $\overline{X_i}$: mean of i^{th} level of factor A; $\bar{X}_j$: mean of the j^{th} level of factor B; and $\bar{X}_{ij}$: mean of cell ij. The factors A and B are assessed for their variance and also any interaction between them using Equations (3)–(7).

In the present study, data from prior studies were assessed as a reference in **Exhibit 4** to construct the influence of meteorological parameters is used on aerosol pollutants and elemental species using a Pearson correlation matrix for the entire sampling phase, while bivariate polar plots were constructed with the openair package in the R programming environment to assess the directionality of potential local pollutant sources concerning wind direction and wind speed (Bodor et al., 2020). Identification of probable metal sources in aerosol was assessed using the positive matrix factorization (PMF) method in PMF 5.0 developed by the United States Environmental Protection

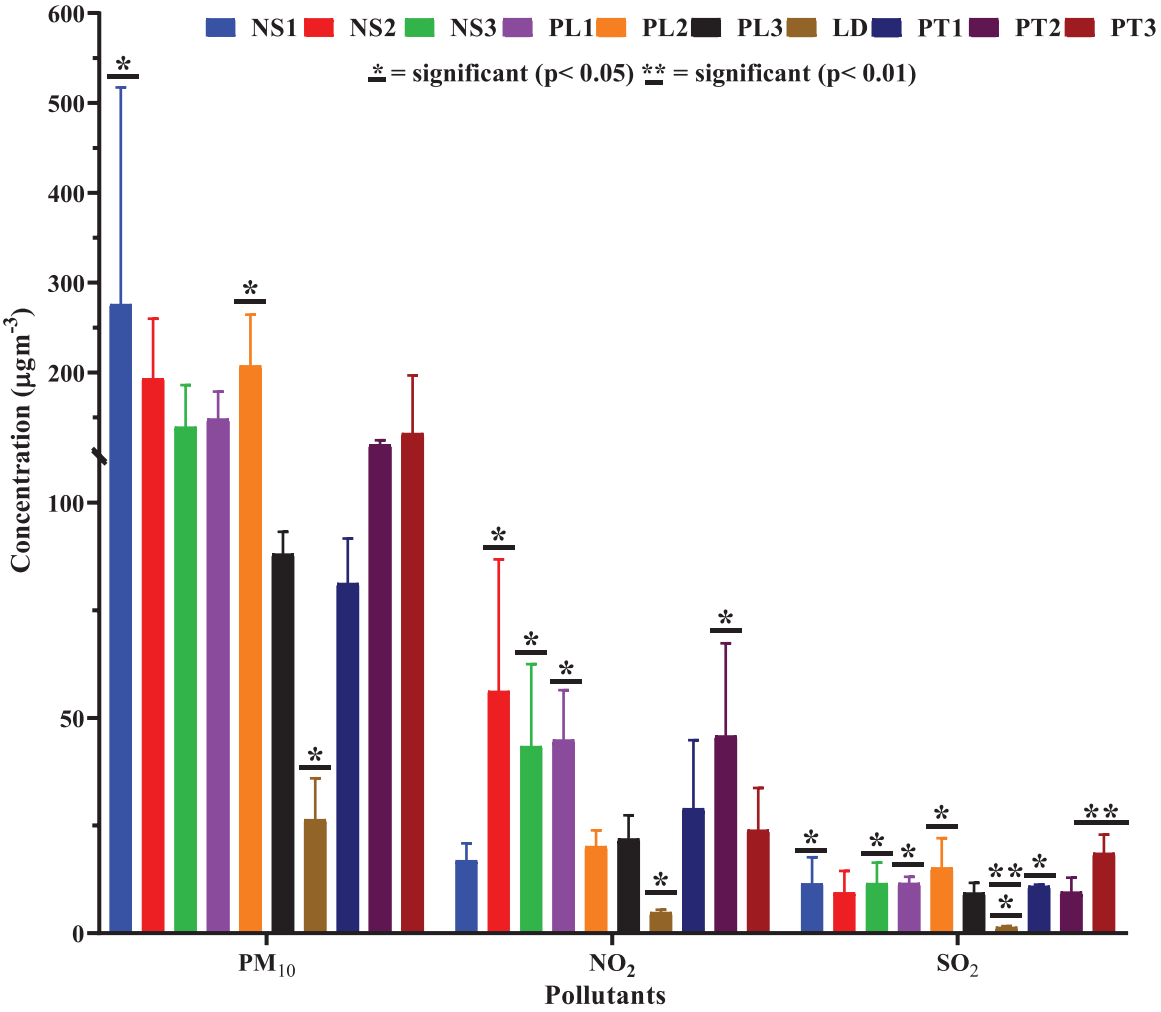

EXHIBIT 2 Mean concentration levels of PM_{10}, NO_2, and SO_2 in aerosol during normal (NS1, NS2, NS3), pre-lockdown (PL1, PL2, PL3), lockdown (LD), and post-lockdown (PT1, PT2, PT3) sampling phase [Color figure can be viewed at wileyonlinelibrary.com]

Agency (USEPA), where the data matrix along with the uncertainty of each sample was calculated using the process stipulated by Reff et al. (2007), considering the method detection limit of concentration values (Yu et al., 2013).

The apportionment of different elemental species was carried out referring to the formulas (Equations 8 and 9) in a study by Jain et al. (2017), which describes the various components required in the identification of pollutant sources of a given data matrix. The data matrix was analysed using the following formula:

$$e_{ij}X_{ij} - \sum_{k=1}^{p} g_{ik}\, f_{kj} \tag{8}$$

$$Q = \sum_{i=1}^{n}\sum_{j=1}^{m}\left[\frac{e_{ij}}{u_{ij}}\right]^2 \tag{9}$$

where, X_{ij}: data matrix with a dimension of i (number of samples) by j (concentration of element species), g: magnitude of the mass contribution of each sample by each factor, p: number of factors, f: species fraction, and e_{ij}: residual species in sample i, Q: object function, u_{ij} : uncertainty of j element species of i sample in the matrix.

The above-mentioned formulas were utilized to achieve an optimum data matrix and their corresponding source profile. To achieve the optimum conditions the model was run 20 times with six factors for each dataset. A hundred bootstrap-per operation was performed with a minimum r^2 value at 0.6. Rotation of the base factor for each run was carried out through modulating Fpeak values between −0.5 and 1.5 to find an optimum source for each metal species. The source apportionment of each metal species was confirmed by comparing estimated values with previous references and their strength was estimated using S/N ratio values as illustrated in the supplementary file (Figure SF3). The interpretation and graphical representation of the results were done on actual data using Graphpad Prism version 8.0.2.

3 | RESULT AND DISCUSSION

3.1 | Meteorological study

The distinctive onset of monsoon seasons categorized the sampling site to have a tropical climate under the Köppen climate classification

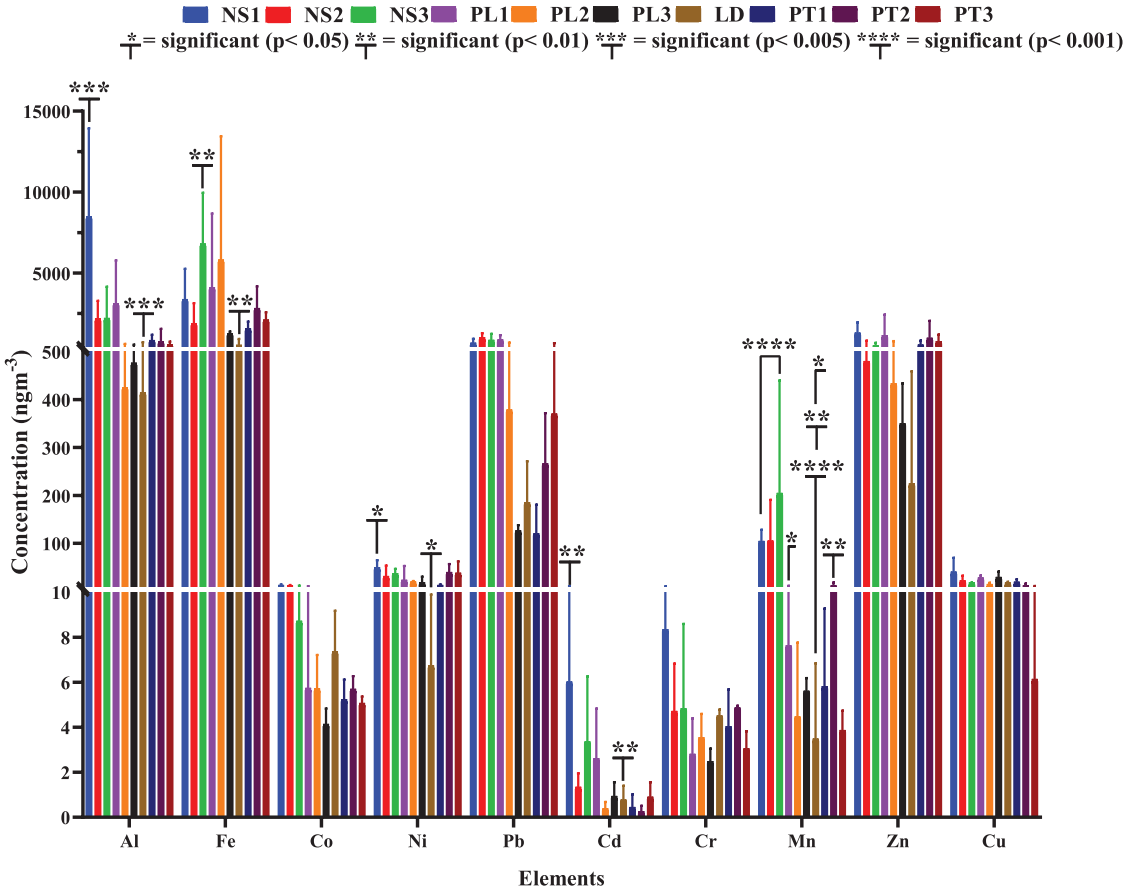

EXHIBIT 3 Mean concentration levels of elements in aerosol during normal (NS1, NS2, NS3), pre-lockdown (PL1, PL2, PL3), lockdown (LD), and post-lockdown (PT1, PT2, PT3) sampling phase [Color figure can be viewed at wileyonlinelibrary.com]

which is also described in a prior study by Gupta et al. (2008). The seasonal trend of the entire sampling phase can be categorized into four distinct seasons, winter (NS1-3 and PT2-3), spring (PL1-3), summer (LD) and monsoon (PT1) (Karar et al., 2006). The mean temperature during the entire sampling phase was 24.81±3.78°C, while respective sampling phases were observed to be NS (24.05±3.44°C), PL (21.51±3.63°C), LD (29.46±1.79°C) and PT (27.15±2.53°C), respectively. The winter months in Kolkata as mentioned in a study by Diong et al. (2016), is prone to have the highest concentration levels of pollutants due to the inversion layer convecting closer to the ground (Gupta et al., 2008). This phenomenon was observed during NS and PT phases as represented in Exhibit 2, where the concentration levels for PM_{10} were observed to be higher in comparison to the LD phase.

The average relative humidity (rh) during the study period was recorded to be 73.81±11.61%, ranging between 60 and 90%. The mean rh during the LD phase was found to be 86.11±10.05%, which favor higher mixing potential and disintegration of PM_{10} into smaller particles when subjected to relatively higher ambient temperature (Gogikar et al., 2018), thus reducing overall pollution load. The city during the NS and PT phases predominantly experienced the north-westerly winds with an average speed of 0.35±0.16 ms^{-1} initiating the condition of stagnation and rise in pollution load (Gogikar et al., 2018), while the LD sampling phase was dominated by south-westerly winds blowing in an average of 0.49±0.16 ms^{-1} arising from the Bay of Bengal and Arabian sea (Majumdar et al., 2020), causing a sea-based disturbance and with ventilation potential resulted in a reduction in pollutant concentrations (Gupta et al., 2006; Karar et al., 2006). As meteorological conditions play a pivotal role in the dynamics of pollutant dispersion, the aerosol in the sampling site during LD was found to be dominated by PM_{10} as illustrated in Exhibit 2, while the higher PM_{10}/ NO_2 ratio in the aerosol indicates towards emission from the vehicular source (Biswas & Ayantika, 2021), as average wind speed during sampling timeline did not exceed 1.0 ms^{-1}, thus confirming higher probability of pollution source to be near the sampling site (Gogikar et al., 2018). The seasonal variation of pollutants at the sampling site followed the trend of higher concentration levels during NS and PT followed by the PL sampling phase, while a large reduction during the LD phase was observed due to the combined effect of atmospheric dynamics and anthropogenic activities (Singh et al., 2020).

3.2 | Particulate matter

The mean concentration levels of PM_{10}, NO_2, and SO_2 during different sampling phases are illustrated in Exhibit 2, while the elemental profile of PM_{10} is illustrated in Exhibit 3. The mean concentration value

EXHIBIT 4 Seasonal variation of aerosol elemental profile in Kolkata in comparison with other prior studies

Reference	Study Area	Sampling timeline	Particulate concentration range (μgm^{-3}) PM_{10}	Elemental concentration range (ngm^{-3})											
				Fe	Pb	Cr	Cd	Zn	Ni	Co	Al	Mn	Cu	Phase	Season
This study	Kolkata, India	October 2019–November 2020	82.17–546.21	960–9032	465.3–1318.7	2.29–10.12	0.28–11.45	194.8–1821	12.3–67.1	5.3–13.9	951.7–12022.5	2.3–463.4	11.7–72.11	NS (1–3)	Winter
			82.15–272.06	1174–14625	116.9–1072.1	1.52–4.62	0.02–4.54	30.7–2632	0.01–56.41	1.6–11.25	257.7–5680.7	1.9–11.7	9.95–41.26	PL (1–3)	Spring
			17.51–36.53	318.9–987.12	130.1–284.2	4.28–4.83	0.03–1.15	78.9–495.2	3.9–10.14	5.25–8.59	58.38–661.05	0.02–6.75	1462–19.03	LD	Summer
			60.61–186.77	1059.7–4356.1	57.1–718	2.12–5.06	0.01–1.64	17.96–2138.4	10.6–65	4.71–6.32	161.9–1667.4	2.3–19.6	0.82–25.86	PT (1–3)	Monsoon, Winter
Karar et al. (2006)	Kolkata, India	November 2003–November 2004	159.4–232.3	116.7–144.9	66.9–244.4	4.4–8.4	4.8–6.5	407.3–452.2	6.4–7.3	***	***	3.7–3.8	***	***	Winter
			166.7–291.9	102.6–144.2	49.7–134	8.3–13.7	3.5–4.1	309.8–613.8	9.5–10.4	***	***	1.2–2.1	***	***	Spring
			135.1–154.3	52–89.2	18.5–41.5	3.2–7.2	1.8–2.5	542.2–646.6	4.5–7.7	***	***	1.9–2.1	***	***	Summer
			95.5–107.7	62.1–106.5	17.3–40.1	4.3–5.7	1.2–5.2	451.3–587.9	5.2–8	***	***	1.7–2.1	***	***	Monsoon
Gajghate et al. (2005)	Kolkata, India	January –December 2001	132–219	127–429	131.0–449	3.0–8.0	4.0–15	3753–6870	12–1508	***	***	***	***	***	Winter
			91–154	3.0–615	97–716	8.0–19	6.0–43	30–869	9.0–28	***	***	***	***	***	Summer
			58–92	3.0–138	3.0–210	4.0–19	3.0–77	3.0–209	5.0–20	***	***	***	***	***	Monsoon
			88–143	***	***	***	***	***	***	***	***	***	***	***	Post-monsoon
Prabakaran and Manikandan (2018)	Chennai, India	July 2017–June 2018	***	***	20–991	***	***	***	51–3431	***	***	***	***	***	Pre-monsoon
			***	***	15–1032	***	***	***	2.0–1250	***	***	***	***	***	Monsoon
			***	***	1.0–1035	***	***	***	36–3255	***	***	***	***	***	Post-monsoon
			***	***	125–1854	***	***	***	5.0–4325	***	***	***	***	***	Summer
EzhilKumar et al. (2021)	Chennai, India	January–February 2020	22–180	223–909	31.5–188	2.6–62.6	***	462–4570	0.2–22.1	***	446–2930	52.3–119	8.7–69.4	***	Winter
Parvizimehr et al. (2020)	Shiraz, Iran	September–December 2018	73–230	453–2030	2.43–19.5	0.56–6.44	0.05–0.670	7.78–202	1.0–8.36	***	173–1136	***	***	***	Autumn
Majumdar et al. (2020)	Kolkata, India	July–October 2019	42–69	250–648	2.3–36.0	1.4–2.8	0.1–1.0	18.0–129.0	1.1–8.4	***	260–893	6.9–25	1.4–6.3	***	Monsoon

*** - Data unavailable.

Abbreviations: NS, Normal sampling; PL, Pre-lockdown; LD, Lockdown; PT, Post-lockdown.

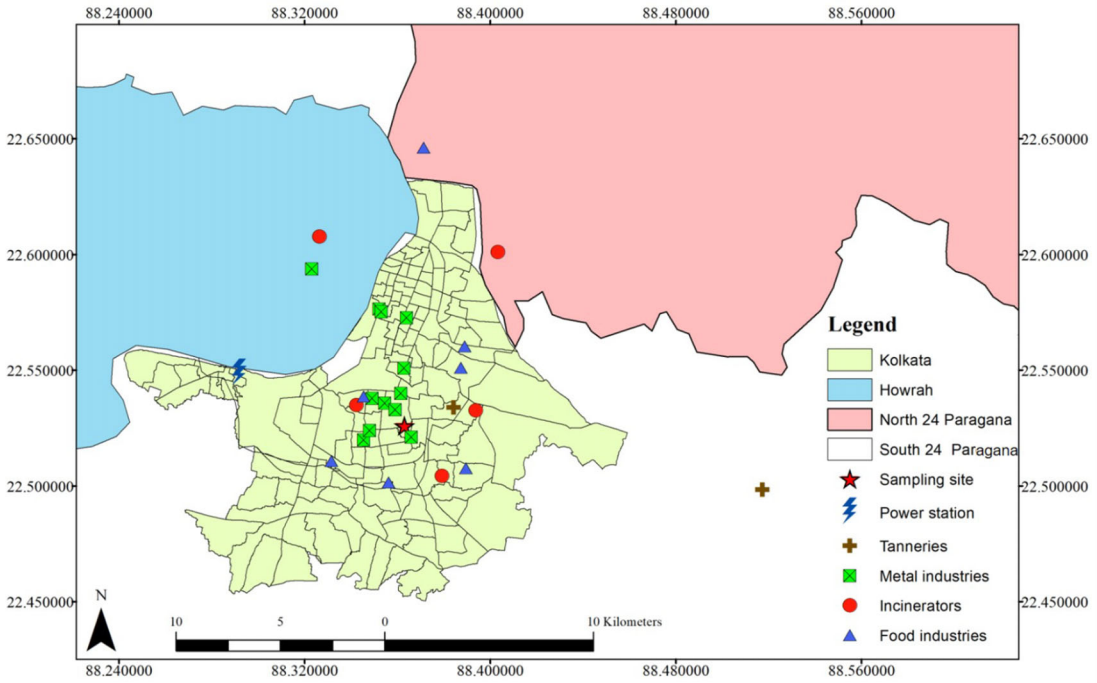

EXHIBIT 5 The map illustrates the major pollutant contributors located in Kolkata Municipal Corporation, North 24 Paragana, and South 24 Paragana administrative areas [Color figure can be viewed at wileyonlinelibrary.com]

of PM_{10} during the study phase was observed to be 141.1±71μgm^{-3}, while it was observed that in the study area mean PM_{10} concentration reduced by 86.97%, 82.12% and 76.19% during the lockdown in comparison to the NS, PL and PT phase, respectively. The LD phase was observed to have the PM_{10} concentration range from 17.51 to 36.53 μgm^{-3}, which corresponds to a reduction of −82.12%. This reduction is mainly influenced by the combined effect from the higher mixing layer, low anthropogenic activities (Sarkar et al., 2021) and disintegration of PM_{10} into smaller particles (Gogikar et al., 2018). The NS, PL and PT sampling phase exhibited the concentration level range of 82.17-546.21 μgm^{-3}, 82.15-272.06 μgm^{-3} and 60.61-186.77 μgm^{-3}, respectively, where the concentration levels during NS and PT were found to be mainly contributed from clusters of small industries (Kabiraj & Gavli, 2020), tanneries (Sarkar et al., 2021), thermal power plant (Biswas & Ayantika, 2021) and vehicular emissions (Banerji & Mitra, 2021).

The Ballygunge as described in a study by Sarkar et al. (2021), experiences poor ambient air quality as pollutant loads from major emission sources as illustrated in **Exhibit 5** tend to accumulate in the lower mixing layer further complementing the traffic emission extensively (Bodor et al., 2020). The bivariate polar plots in Exhibits 6 and 7 present the directionality of major emission sources contributing to frequent pollutant load in the sampling site. The major contributors of PM_{10} during the NS phase were identified as small-scale industrial complexes in the southwestern part of Kolkata, while the coal-based power plant in the northwestern direction from the sampling site was found to have a significant contribution.

In **Exhibit 6(b)**, the major contributors during the PL phase were quantified to be the vehicular emissions from adjacent road junctions and metal industries located nearby, while in the LD phase as illustrated in **Exhibit 7(c)**, the significant contributor of PM_{10} was incinerator which operational to process local solid wastes. The contributions during the PT sampling phase were observed to be dynamic as the relaxation was granted to the population with some exceptional areas where high COVID-19 cases were observed. The major contributors in the PT sampling phase were identified as metal processing units, food industries, and incinerators located in the southern part of Kolkata.

The bivariate plots for PM_{10} in Exhibits 6 and 7 indicated that pollutant sources at the sampling site were predominantly emitted from the vehicular exhaust as a high PM_{10}/ NO_2 ratio in the aerosol was observed and the average wind speed throughout the sampling phase was less than 2 ms^{-1} (Gogikar et al., 2018), which is a prime factor that favors the stagnation of the pollutants from a nearby road junction as in this case.

3.3 | Gaseous pollutants

The mean concentration value of NO_2 and SO_2 during the entire study phase was observed to be 30.70±16.13 μgm^{-3} and 10.91±4.41 μgm^{-3}, respectively. The observed values for the reduction in the mean concentration of NO_2 and SO_2 were (87.61%, 83.38%) and (87.36%, 88.60%) during the lockdown phase in comparison to the NS and PL sampling phase respectively. The LOD for gaseous pollutants (SO_2 and NO_2) was estimated to be 1400 μgm^{-3} and 200 μgm^{-3} respectively, whereas the LOQ was estimated to be 4000 μgm^{-3} and 700 μgm^{-3} respectively, which was found to be in the working range

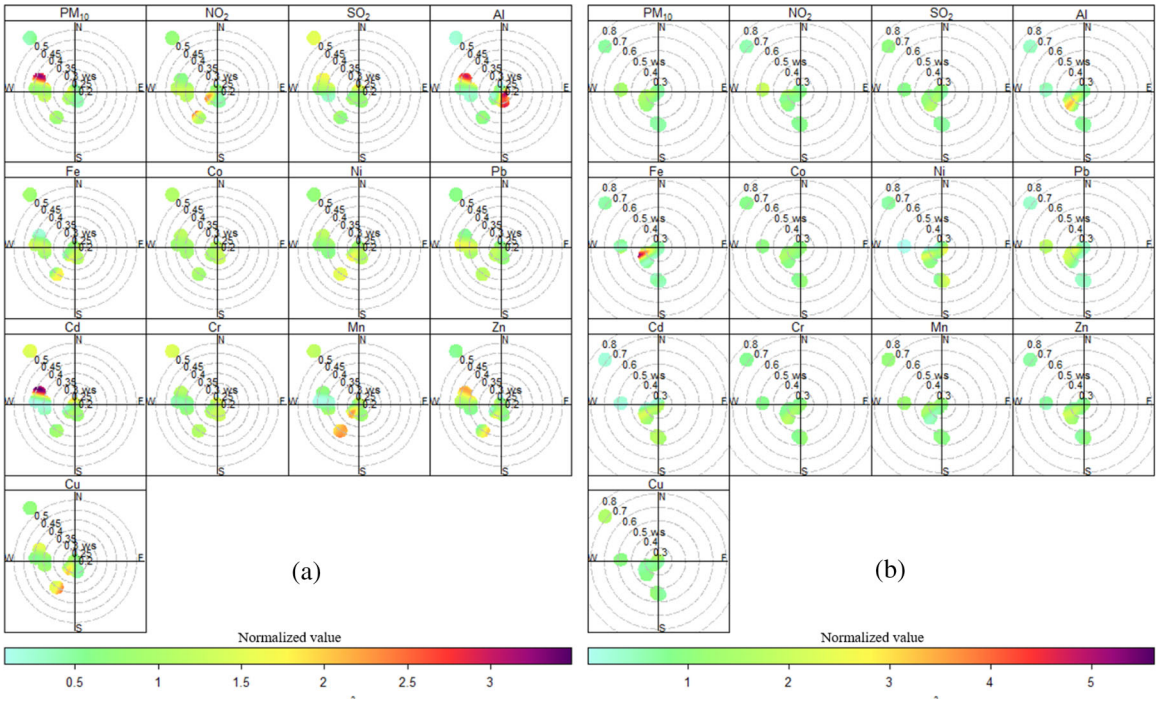

EXHIBIT 6 Bivariate polar plot of elements in aerosol during: (a) normal and (b) pre-lockdown sampling phase [Color figure can be viewed at wileyonlinelibrary.com]

(3–2000 μgm^{-3} to 10000 μgm^{-3}) as prescribed in the study by Villanueva et al. (2021).

A positive association between PM_{10}/NO_2 ($r = 0.21$) and PM_{10}/SO_2 ($r = 0.40$) in **Exhibit 8**, during the same phase, implies that PM_{10} and NO_2 are emitted from the vehicular source, mainly due to a significant concentration level of NO_2 in comparison to SO_2 in the ambient air (Dimitriou & Kassomenos, 2017). The relative association between NO_2 and SO_2 during the entire sampling phase infers that they are emitted from two different sources, as discussed in the previous section. The bivariate polar plot in Exhibit 6(a) presents the major emission source in the NS sampling phase for NO_2 to be vehicular emissions from traffic junction adjacent to the sampling site (Gogikar et al., 2018), while for SO_2 the higher concentration can be observed at the northwestern part of Kolkata which is known to harbor the coal-based power station as presented in Exhibit 5, thus implying the emission source to be the thermal power station (Biswas & Ayantika, 2021). The directionality of NO_2 and SO_2 during the PL sampling phase was observed to be clustered around the center (sampling site) with minor contributions from metal processing units located in the west of the sampling site resulting in the accumulation of pollutants under low wind speed and lower mixing layer as described in a study by Bodor et al. (2020), regarding the transportation of pollutants in the urban environment.

The back-trajectories analysis of winds during different sampling phases as illustrated in **Exhibit 9** and supplementary file (Figures SF4–SF6) presented that prominent air parcels during the NS, PL, LD and PT were in northeasterly; southerly, south-easterly and northerly direction, respectively. These air parcels were incorporated to identify emission sources during the LD sampling phase, which in Exhibit 9 can be observed to be predominately from the Bay of Bengal arriving at heights of 500–1500 meters above ground level (agl) which are presumed to be low in particulate matter (Gogikar et al., 2018). These air parcels initiate a higher mixing rate which leads to a reduction in pollution load as observed during the LD phase. The combined effect of higher mixing rate with clean air parcel and restriction on anthropogenic activities due to COVID-19 lockdown reduced the NO_2 and SO_2 concentration levels below the permissible limit (80 μgm^{-3}) as per National Ambient Air Quality Standards (NAAQS) (CPCB, 2013). The potential sources as propounded using polar plot were observed to be identical to these trajectories, where the contributions from vehicular emission, metal industries (Gajghate et al., 2005) and incinerators as illustrated in **Exhibit 10**, dominated concurrently during NS, PL and PT sampling phase. On the contrary, during the LD phase the major contributors were vehicular emissions and an incinerator (Biswas & Ayantika, 2021).

3.4 | Metal concentrations

The assessment for the abundance of each elemental species observed during the respective sampling phase is represented in the order of their mean concentration as followed:

1. NS phase: Fe (3314.4 ngm^{-3}) > Al (2185.37 ngm^{-3}) > Pb (792.85 ngm^{-3}) > Zn (531.72ngm^{-3}) > Mn (105.25 ngm-^{3}) > Ni

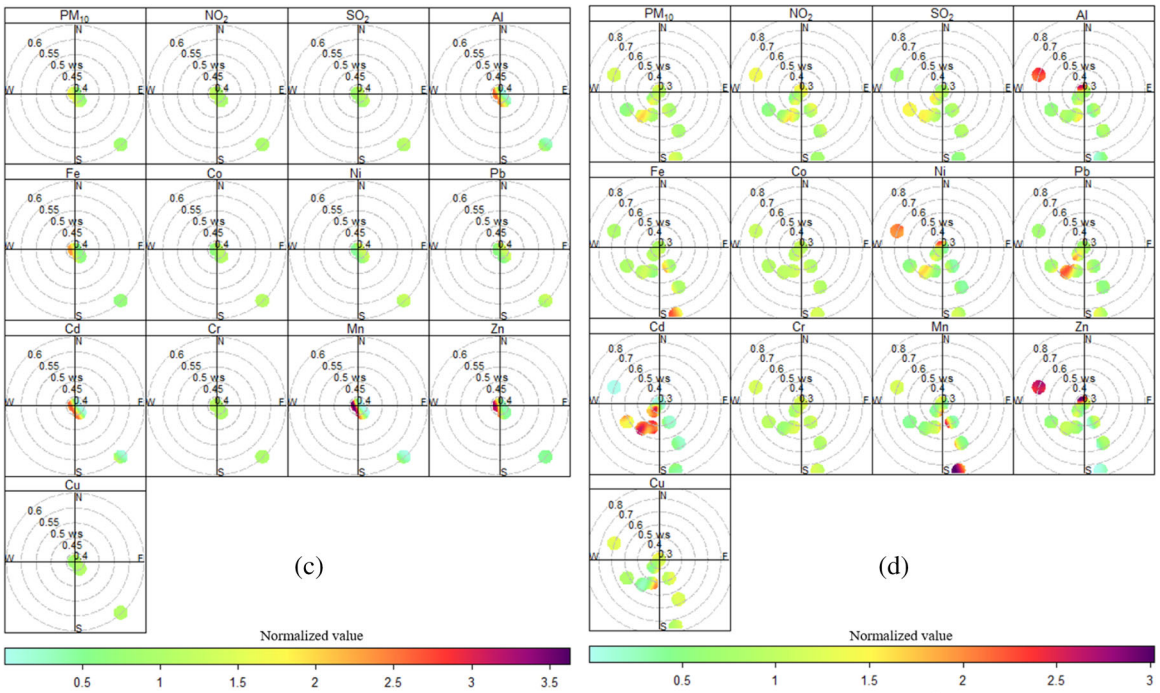

EXHIBIT 7 Bivariate polar plot of elements in aerosol during (c) lockdown and (d) post-lockdown sampling phase [Color figure can be viewed at wileyonlinelibrary.com]

(39.58 ngm^{-3}) > Cu (18.46ngm^{-3}) > Co (11.41ngm^{-3}) > Cr (6.7ngm^{-3}) > Cd (3.15ngm^{-3}).

2. PL phase: Fe (1407.9 ngm^{-3}) > Al (514.295 ngm^{-3}) > Zn (447.25 ngm^{-3}) > Pb (270.7 ngm^{-3}) > Cu (23.95 ngm^{-3}) > Ni (17.84 ngm^{-3}) > Mn (5.32 ngm^{-3}) > Co (4.43 ngm^{-3}) > Cr (2.5 ngm^{-3}) > Cd (0.56 ngm^{-3}).
3. LD phase: Al (522.14 ngm^{-3}) > Fe (322.51 ngm^{-3}) > Pb (139.5 ngm^{-3}) > Zn (98.51 ngm^{-3}) > Cu (18.51 ngm^{-3}) > Co (8.21 ngm^{-3}) > Ni (6.14 ngm^{-3}) > Cr (4.39 ngm^{-3}) > Mn (3.65 ngm^{-3}) > Cd (1.11 ngm^{-3}).
4. PT phase: Fe (1841.3 ngm^{-3}) > Al (555.78 ngm^{-3}) > Zn (514.97 ngm^{-3}) > Pb (179.2 ngm^{-3}) > Ni (26.12 ngm^{-3}) > Cu (11.55 ngm^{-3}) > Co (5.19 ngm^{-3}) > Mn (5.81 ngm^{-3}) > Cr (4.76 ngm^{-3}) > Cd (0.4 ngm^{-3}).

Complementary to the abundance of elemental species, the mean concentration of each element during different sampling phases is illustrated in Exhibit 3. The reduction in observed mean concentration of metals during lockdown were in the following order: Mn (97.47%) > Al (90.33%) > Fe (86.38%) > Ni (82.77%) > Cd (78.57%) > Pb (78.06%) > Zn (70.38%) > Cu (34.54%) > Co (31.50%) > Cr (24.39%), when compared with the mean metal concentration for normal sampling phase. Similarly, when comparing with mean concentration of pre-lockdown phase the reduction for each metal was in the following order: Fe (85.31%) > Al (69.08%) > Ni (66.51%) > Zn (65.7%) > Pb (59.71%) > Cd (41.43%) > Mn (41.02%) > Cu (26.16%). From Exhibit 8, a significant association between Fe with Pb (r = 0.57) was observed, indicating that they originate from the same source (Jeričević et al., 2019). The intercorrelation between element and pollutants recommends the homogenous potential pollution sources and are explained in their respective sections.

3.5 | Source apportionment of elements

In this study, profiling of elemental sources using the PMF-based method on the dataset was conducted by comparing estimated values and major elemental markers from previous references as shown in **Exhibit 11**. The elemental species were categorized according to their signal-to-noise (S/N) ratio, where species with values less than 0.5 were considered as bad whereas, species with values greater than 0.5 but less than 1 were considered as good and values greater than 1 were considered as strong species for that sampling phase (Rajput et al., 2016). The S/N ratio of all elemental species was calculated using PMF 5.0 for each sampling phase and the acquired values suggested that all elemental species except Cd were strong. The S/N ratio of each element is represented in the supplementary data (Figure SF3). The profiling of all elemental sources was carried out using the S/N ratio value to identify the strong classified elements in comparison with source profiles from prior studies along with meteorological conditions during the sampling phase. The optimization of factors was carried out by comparing the $Q_{actual}/Q_{expected}$ values for different factors and was observed that there was a slight decrease in Q-value between six factors and seven factors solution (7.28 to 6.88). In contrast, there was a larger decrease in Q-value when five factors solution was compared with six factors solution (8.49–7.28). This slight decrease suggested that a solution with six factors was optimum for analysis (Brown et al., 2015).

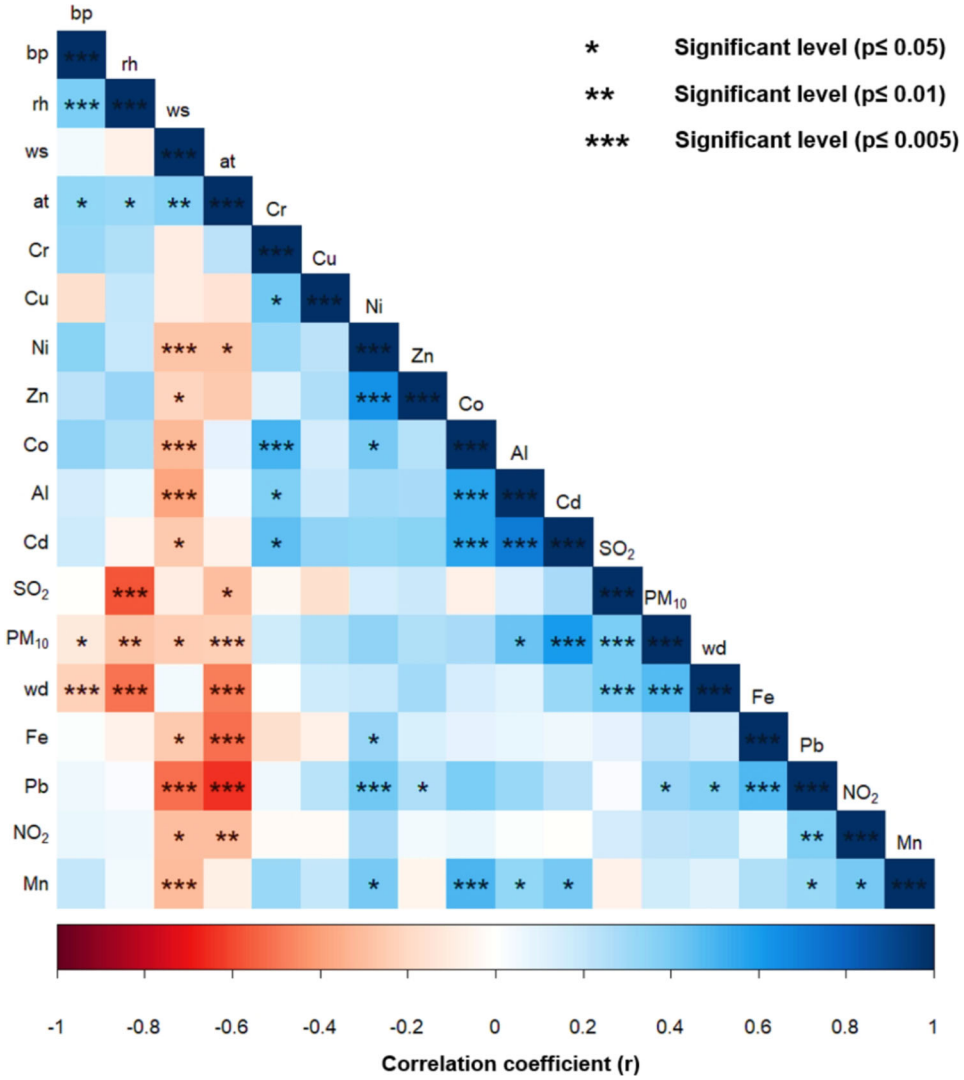

EXHIBIT 8 Correlational matrix of pollutants, meteorological parameters and elements in aerosol during the sampling phase [Color figure can be viewed at wileyonlinelibrary.com]

Identified source profiles according to their contribution to total PM_{10} mass concentration were soil/resuspended dust (Mousavi et al., 2018), coal combustion (Gajghate et al., 2005), industrial emission (Karar et al., 2006), vehicular emission (Gu et al., 2011), leather tanneries (Rajput et al., 2016) and incinerators (Gajghate et al., 2012). The identified profiles were further complemented by the HYSPLIT model by analyzing the air parcels arriving at heights of 500, 1000 and 1500 m during the lockdown as illustrated in Exhibit 9. The dominating winds were mainly originating from the Arabian Sea and the Bay of Bengal, which tend to carry cleaner air and get contaminated as they approach the urban industrial areas, like Kolkata (Gogikar et al., 2018). This condition favors the assessment of variation in pollutants and their potential source profile as air columns are trapped into atmospheric inversion (Moreno et al., 2006). The percentage contribution of each metal species that are estimated for source profiling during different sampling phases is discussed in the following sections and graphically presented in **Exhibit 12** and 13, while detailed information is supplied in the supplementary file (ST2–ST5).

The first factor of PMF analysis is identified as soil and resuspended dust particles which is one of the major contributors to total PM_{10} load in the aerosol of the Kolkata metropolitan area during the NS phase (30.64% of total contribution percentage), supplemented predominantly from heavy traffic loads and construction activities. The percentage contribution of soil/resuspended dust gradually diminished to 14.15%, 16.52%, and 16.15% during the PL, LD and PT sampling phase, respectively, as illustrated in Exhibit 10, which indicates the impact of sudden lockdown and restriction to anthropogenic activities resulted in reduced degradation of unpaved roads (Yu et al., 2013). The major contributing elements during the entire sampling phase were estimated in the following order Al (60.5%), Cd (52.4%), Cr (44.5%) and Fe (28.8%), which are mainly emitted from the earth crust and unpaved roads by ongoing traffic, while the concentration level of Al was observed to be high during the LD sampling phase due to its abundance in earth crust which tends to get resuspended in form of dust particles, whereas other metals like Mn, Cu, and Cr were observed to be present in lower concentration levels mainly generated from

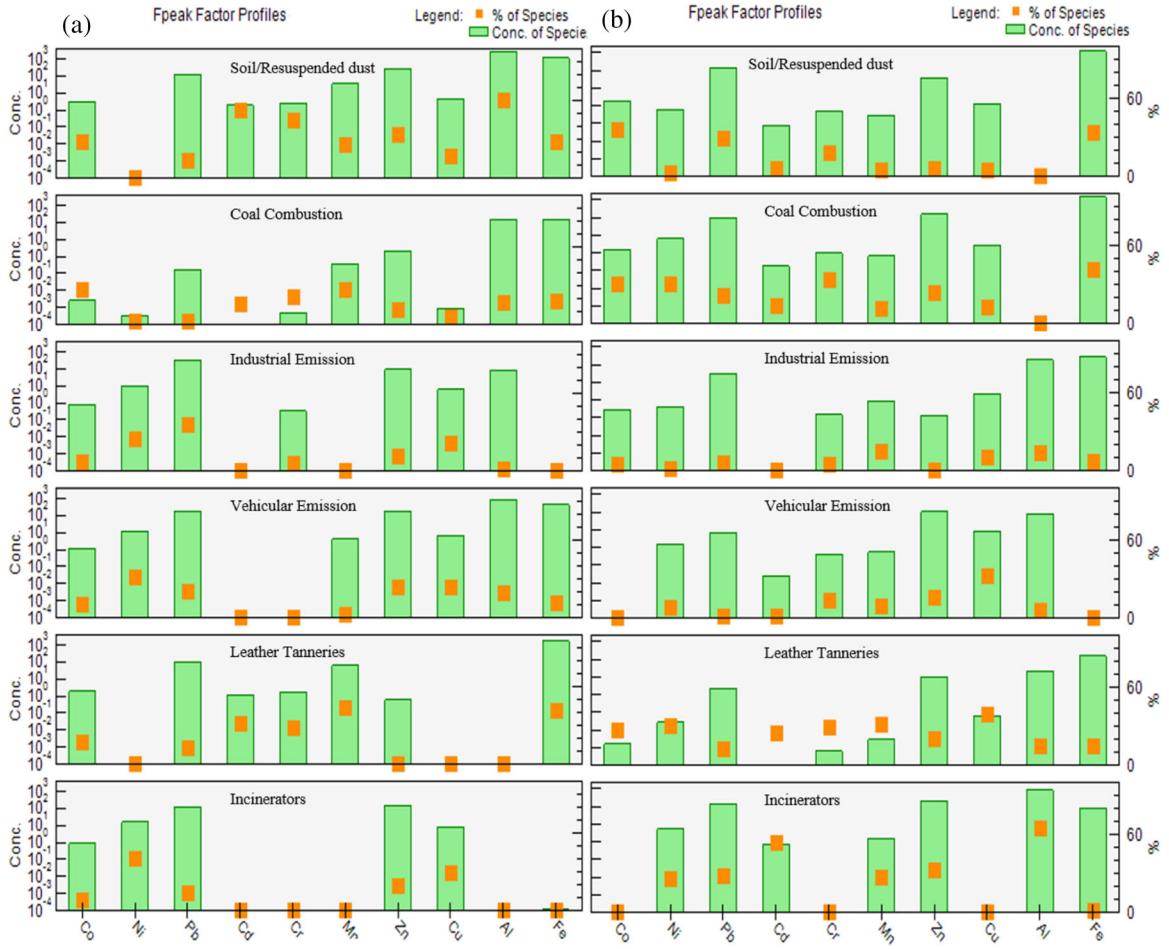

EXHIBIT 10 Average percentages of source profile in aerosol during normal (NS), pre-lockdown (PL), lockdown (LD) and post-lockdown (PT) sampling phase [Color figure can be viewed at wileyonlinelibrary.com]

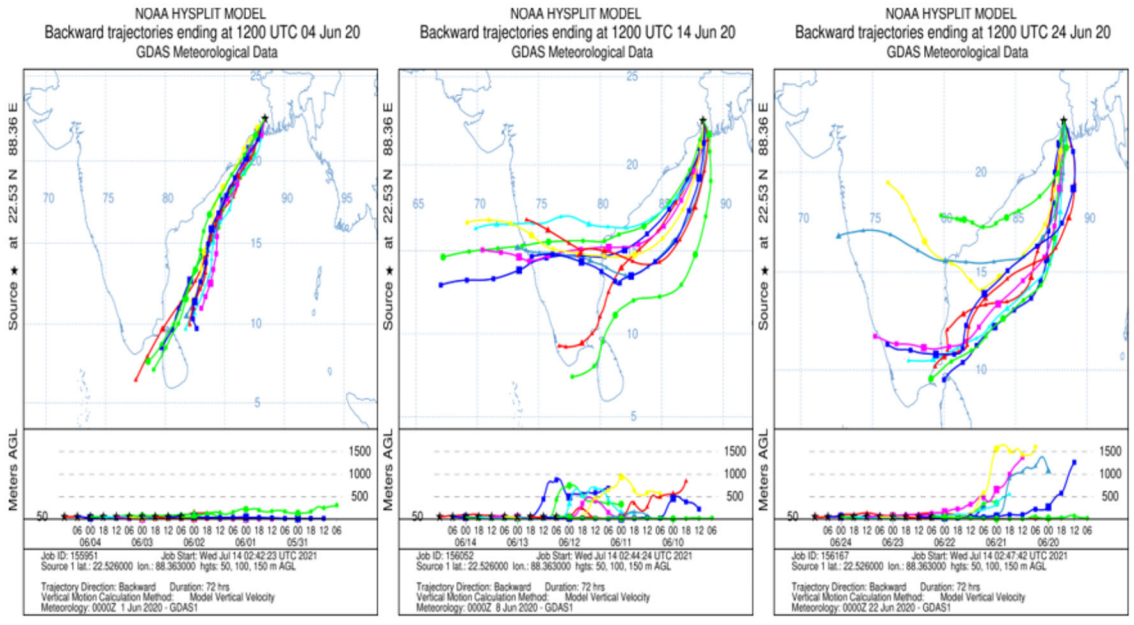

EXHIBIT 9 Back-trajectories illustrating the movement of air parcels during the lockdown sampling phase [Color figure can be viewed at wileyonlinelibrary.com]

EXHIBIT 11 Studies on the identification of metal sources from aerosol using various apportionment methods

Reference	Year	Source Apportionment Method	Number of the source profile	Metals
This study		Positive matrix factorization	6	Cr, Al, Zn, Fe, Mn, Co, Cu, Pb, Ni, and Cd
Guo et al. (2009)	2009	Principal component analysis	5	Al, Si, Se, K, Mg, V, Zn, Ti, Pb, Ni, Mn, Na, Ca and Fe
Yu et al. (2013)	2013	Positive matrix factorization	7	Mg, Al, Si, P, S, Cl, K, Ca, Ti, v, Cr, Mn, Fe, Ni, Cu, Zn, As, Se, Br, Ba, and Pb
Jeričević et al. (2019)	2019	Positive matrix factorization and conditional Probability Function	5	Ca, Cu, Na, Mn, Mg, V, Cr, Zn and Co
Rajput et al. (2016)	2016	Positive matrix factorization	6	Na, K, Ca, Fe, Mg, As, Cd, Cr, Cu, Ni, Pb, Se, V, Zn, and Mn
Karanasiou et al. (2009)	2009	Positive matrix factorization	6	Cd, Pb, V, Ni, Mn, Cr, Cu, Fe, Al, Ca, Mg, K, and Na
Gu et al. (2011)	2011	Positive matrix factorization	6	Ca, Cd, Ce, Co, Cr, Cu, Fe, K, La, Mg, Mn, Ni, Pb, Sb, Ti, and Zn
Mousavi et al. (2018)	2018	Positive matrix factorization	4	Fe, Cr, Cu, and Mn
Wu et al. (2019)	2019	Principal component analysis	4	Sb, As, Cd, Cr, Pb, Mn, Ni, Se, and Ti
Prati et al. (2000)	2000	Principal component analysis	3	Na, Mg, Al, Si, S, Cl, Ti, V, K, Ca, Cr, Mn, Fe, Ni, Cu, Zn Br, Sr and Pb
Kumar et al. (2001)	2001	Chemical mass balance model	5	Al, As, Ca, Cr, Cu, Fe, Hg, K, Mg, Mn, Na, Ni, and Pb
Larson et al. (2004)	2004	Positive matrix factorization	8	Al, Si, S, Cl, K, Ca, Ti, V, Cr, Mn, Fe, Ni, Cu, Zn, As, Br and Pb
Han et al. (2006)	2006	Positive matrix factorization	14	Al, Si, S, Cl, K, Ca, Ti, V, Cr, Mn, Fe, Ni, Cu, Zn, As, Se, Br, Rb and Pb
Srivastava et al. (2016)	2016	Scanning electron microscope-energy dispersive X-ray, metal marker technique	4	Ba, Cd, Cr, Fe, K, Mg, Na, Mn, Ni, Pb and Zn
Wu et al. (2020)	2020	Partition computing-based positive matrix factorization	4	As, Cd, Cr, Cu, Hg, Ni, Pb, and Zn

eroding asphalt roads as discussed in a study by Jeričević et al. (2019). Likewise, the observed contribution percentage of Pb (19.5%) in aerosol during lockdown can be directly correlated to soil contaminations and its persistence in the soil matrix. The contribution percentage of elemental markers for soil/resuspended dust particles like Fe (0%), Al (22.1%), Cd (9.5%), and Cr (8%) during the LD phase was found to have decreased relatively in comparison to the NS sampling phases as presented in Exhibits 12 and 13, which infers that the higher mixing layer and absence of anthropogenic activities was responsible for the sudden decrease in percentage contributions at the receptor site (Gogikar et al., 2018).

The second identified source for metals in aerosol is emission from the coal-based power plant which is located in the western periphery of Kolkata city as shown in Exhibit 5 and observed to have contributed 15.15%, 22%, 14.94% and 23.98% during NS, PL, LD and PT phase, respectively. Key estimated metal species for source identification of coal combustion along with their corresponding percentage contributions were Ni (2.7%, 30.5%, 15.3%, and 26.9%) and Pb (2.7%, 21.9%, 15.3%, and 30.4%) during NS, PL, LD, and PT sampling phase, respectively (Yu et al., 2013). It was observed that during the LD phase the contribution percentage of the power plant decreased by ~50%, while in the post-lockdown phase it rose back to the pre-lockdown level to support electricity-dependent industries located at different locations in Kolkata city. This variation in elemental contribution percentage mainly corresponds to urban anthropogenic activities like fossil fuel combustion in power plants which mainly emits the elements like Pb, Ni, and Mn into the air as previously described in a study by Kar et al. (2010), which identified the major contributor of these elements in Kolkata. The variation in source profile can be observed from Exhibit 7, wherein 7(c) Pb and Ni are observed to be clustered around the receptor site during the LD sampling phase which later in 7(d) can be observed to have diverged into different emission sources like metal processing unit and power station situated in the southwestern and northwestern side of the receptor site, respectively. This phenomenon is further enhanced due to the stagnation of aerosol in the PT sampling phase mainly due to low temperature and low mixing layers closer to the ground which was also described in a study by Ghermandi et al. (2017).

The third identified source profile is emission from the industrial complexes which corresponds to markers like Mn, Cr and Ni as an elemental footprint in the aerosol (Wu et al., 2019). The percentage contribution of each element was observed to have similar metamorphic tendencies when comparing different phases with each other. The percentage contributions of elemental species were observed to be Mn

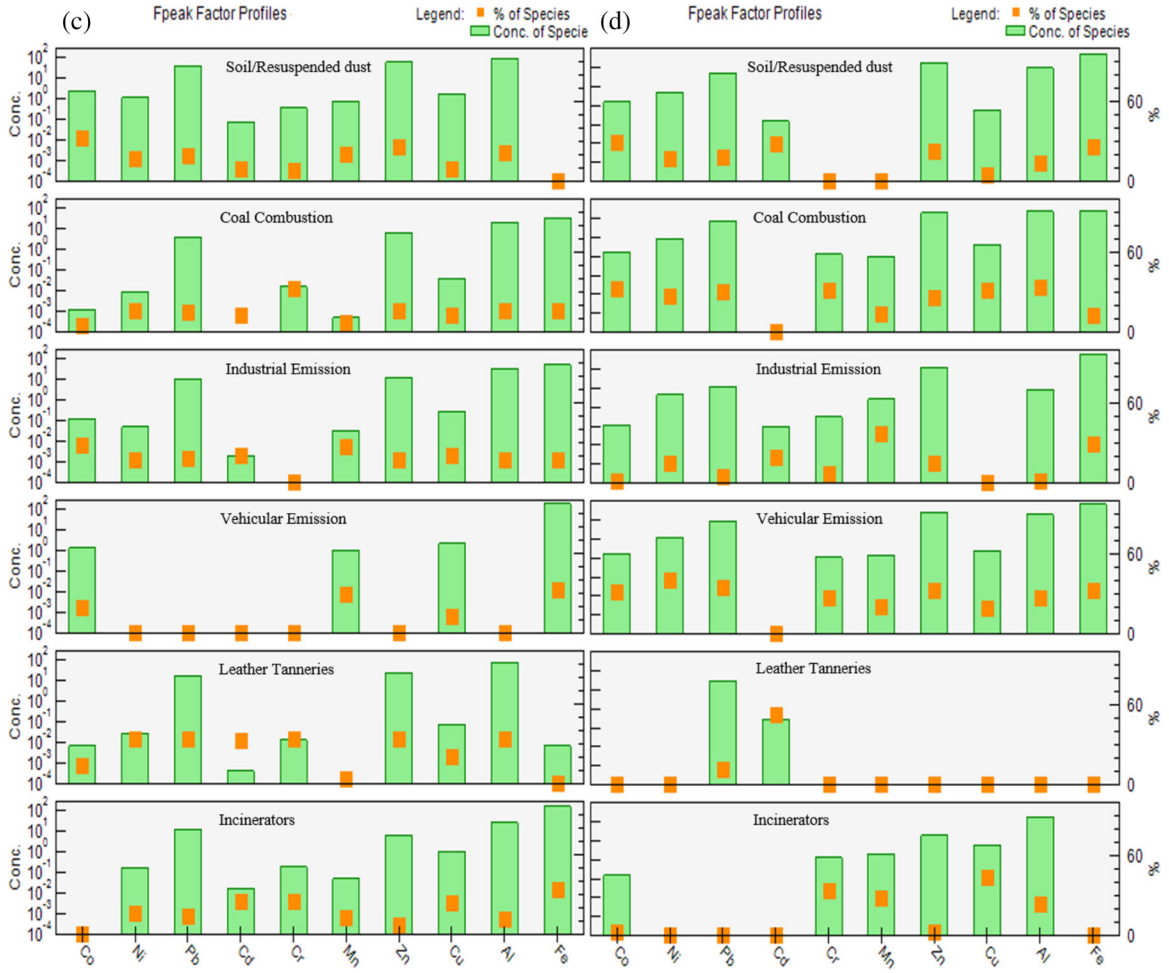

EXHIBIT 12 PMF source profile of metals in aerosol during (a) normal (NS1, NS2, NS3) and (b) pre-lockdown (PL1, PL2, PL3) sampling phase [Color figure can be viewed at wileyonlinelibrary.com]

(14.8%, 26.9%, and 36.9%), Cr (5.2%, 0.5%, and 7.5%) and Ni (2.1%, 17.7%, and 15.2%) during PL, LD, and PT phases, respectively. The consistency in elevated concentration levels of elements from industrial sources during lockdown signifies the emission from food processing units at the south-western direction of the sampling site (Exhibit 5), along with other micro and small industries that were excluded from the embargo during the LD sampling phase. Elevated concentrations levels of Fe and Pb in Exhibit 7(c) suggest that the consistencies in emissions from metal processing units close to the sampling site were prime contributors during the LD phase, whereas the elements like Mn, Ni and Cr are metal markers for the metal processing industry (Kar et al., 2010). The presence of these metals during LD phase indicates that few of these processing units were functional either in the reduced workforce or in various shifts to compensate for the loss due to sudden restrictions.

The fourth source profile is identified as vehicular emission mainly comprising elements like Fe (Guo et al., 2009), Mn (Yu et al., 2013), Co, Zn, Pb (Rajput et al., 2016), Al and V (Shi et al., 2011), identified from Exhibit 11 which comprises of different analytical methods utilized in the identification of elemental markers for aerosol. It was observed in this study that there was a significant reduction in metal concentration load during the LD phase which contributed approximately 9.45% of the total PM_{10} load in the aerosol. An abundance of Fe (33.1%), Mn (29.8%), Co (19%) and Cu (12.3%) in aerosol even during the LD phase suggests their origins to be the oil combustion (Guo et al., 2009), rubber tires (Kar et al., 2010), catalytic converters and dust particles from goods carrying vehicles assigned for transporting the necessary supplies in and out of the city. The Pb here in the study in Exhibits 6 and 7, corresponds to the secondary emission due to wear and tear of the tires that disintegrates the contaminated soil surface as Pb has a long residence time in the environment (Kar et al., 2010). The relaxation in restriction during the PT phase further enhanced the concentrations of these metals in the aerosol, with an average proliferation of ~3.73±0.6% in the contribution percentage.

The fifth emission source is identified as clusters of tanneries close to the sampling site which is known for its contribution towards flourishing commerce and metal load present in the aerosol. The major metal marker for tanneries is Cr along with Fe's significant contribution percentage (Rajput et al., 2016). The estimated percentage of Cr from these sources were 28%, 29%, 33.3% and 0% for NS, PL, LD and PT sampling phases, respectively. The contributions from leather tanneries were found to have a significantly moderate emission

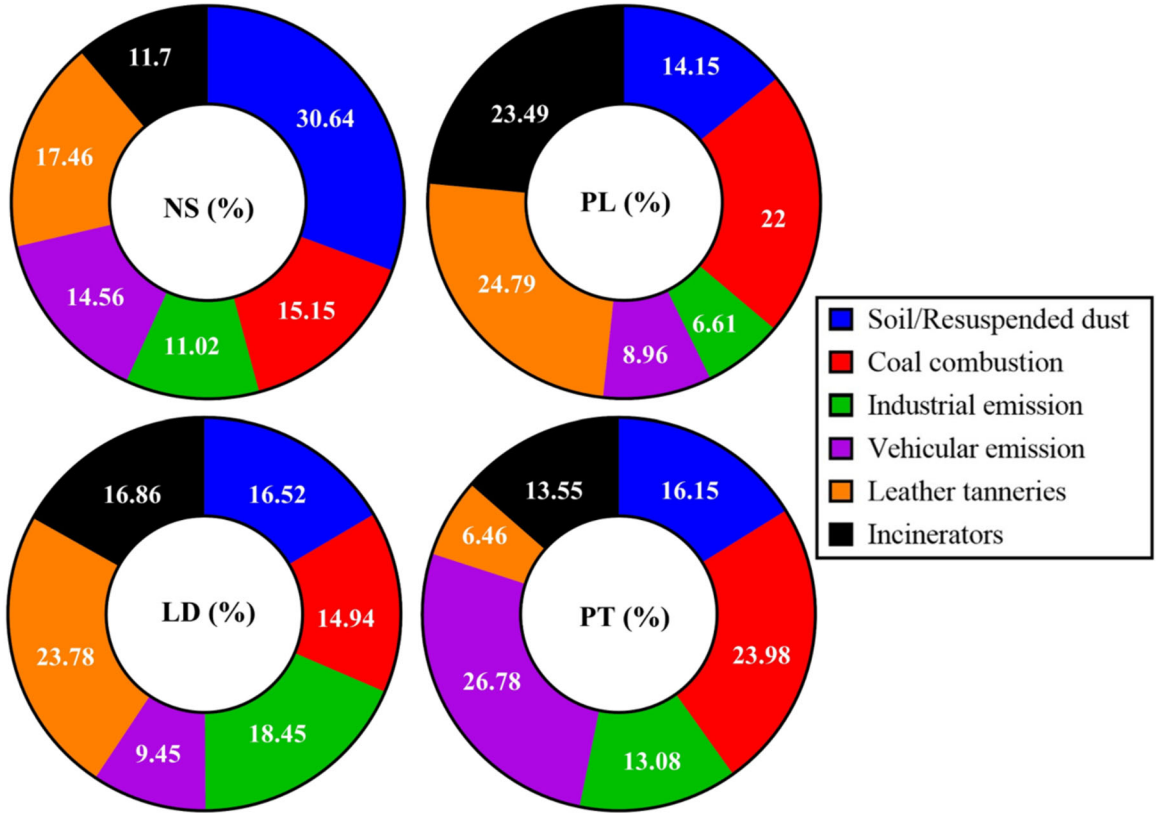

EXHIBIT 13 PMF source profile of metals in aerosol during (c) lockdown (LD) and (d) post-lockdown (PT1, PT2, PT3) sampling phase [Color figure can be viewed at wileyonlinelibrary.com]

percentage in the first three sampling phases: NS (17.46%), PL (24.79%) and LD (23.78%) as illustrated in Exhibit 10. On contrary, during the PT phase, source contribution was found to have reduced to its minimum (6.46%) which must be due to the decreasing market demand with surplus hide products. The emission source during the LD phase can be correlated from Exhibit 7c, that the major pollutants traveled from tanneries located in the south-eastern direction from the sampling site which comprises homegrown processing units.

The sixth source profile is recognized as incinerators which contributed to total PM_{10} load with a fraction of 11.7%, 23.49%, 16.89% and 13.55% during NS, PL, LD and PT, respectively. The significant increase in elemental concentration levels during lockdown at the receptor site was due to the lack of proper waste collection services, which resulted in the flaming of garbage at the dumpsites designated at every residential colony. It was also observed that the mean concentration levels of Cr (3.976 ± 0.0182 ngm^{-3}) and Cd (0.175 ± 0.593 ngm^{-3}) decreased by ~1.45 times during the post-lockdown phase in comparison to the lockdown phase. These improvements in concentration levels are directly related to the ease of restrictions on waste management units, which carried out the disposal of waste more efficiently.

The source apportionment analysis in this study is carried out to find the probable sources following the well-established elemental markers for the identification of secondary pollutants constituting PM_{10} present in the aerosol. The source profiling of PM_{10} according to its elemental constituents helped in validating the elemental variance that occurred due to the COVID-19 lockdown which presented the possibility to quantify the changes in the aerosol. The major finding of this study through PMF modeling is the pollutant trend that is observed between PM_{10} and the elements which were also observed in a prior study by Kar et al. (2010), on the elemental profile of Kolkata city.

4 | CONCLUSION

This study presented the quantified variation in the PM_{10}, NO_2, SO_2 and source apportionment of elemental profiles of the PM_{10} at the Taraknath Palit Siksha Prangan, Ballygunge, a locality in Kolkata city during the nationwide lockdown. The lockdown sampling phase was conducted in the summer season which exhibited the higher temperature and south-westerly winds at the average speed of 0.49 ± 0.16 ms^{-1} arising from the Bay of Bengal and Arabian sea, which favored the higher ventilation potential, which resulted in a reduction in pollutant concentrations in the study area. The observations from this study exhibited that there was an overall reduction in PM_{10} during the lockdown phase, which is observed to be 82.12%, while NO_2 and SO_2 reduced to 87.61% and 87.36% in comparison to the normal sampling phase. The major source of metal species in PM_{10} accounted for soil/resuspended dust emission followed by coal combustions at 19.36% and 19.01%, respectively. The high load of Fe and Al was due to abundance in soil along with the disintegration of vehicular parts

and building materials. Elements during lockdown such as Pb, Ni and Cd were observed to be heavily contributed by the vehicular emission, industrial complexes and tanneries in and around the Kolkata city premise.

The concentration of Pb was found to be elevated throughout the study period implying that it is emitted largely from the soil and automobiles, whereas the reduction in the concentration level of Cd and Cr from incinerators during the post-lockdown phase suggest that due to the inaccessibility of waste management facilities, the population started to incinerate the household waste in the respective local dumpsites. The lockdown facilitated us with the opportunity to evaluate the steps needed for minimizing air pollution through restrictions and its potential to improve air quality on a large scale.

ACKNOWLEDGMENTS

We thank Mr. Ranjan Das and Miss Varsha Sikder for their assistance in sampling processes during tough times. The study was conducted under the project funded by DST-WB, Government of West Bengal under Grant-in-aid (Sanction No.: 290(Sanc.)/ST/P/S&T/10G-33/2017, Date: 28/03/2018).

CONFLICTS OF INTEREST

The author(s) declare(s) that there is no conflict of interest.

DATA AVAILABILITY STATEMENT

All data generated or analyzed during this study are included in this published article (and its supplementary information files).

ORCID

Punarbasu Chaudhuri https://orcid.org/0000-0001-8957-2731

REFERENCES

Banerji, S., & Mitra, D. (2021). Assessment of air quality in Kolkata before and after COVID-19 lockdown. *Geocarto International*, 1–24. https://doi.org/10.1080/10106049.2021.1936209

Barman, S. C., Singh, R., Negi, M. P. S., & Bhargava, S. K. (2009). Fine particles (PM2.5) in ambient air of Lucknow city due to fireworks on Diwali festival. *Journal of Environmental Biology*, *30*(5), 625–632.

Barnett, A. G., Williams, G. M., Schwartz, J., Neller, A. H., Best, T. L., Petroeschevsky, A. L., & Simpson, R. W. (2005). Air pollution and child respiratory health: A case-crossover study in Australia and New Zealand. *American Journal of Respiratory and Critical Care Medicine*, *171*(11), 1272–1278. https://doi.org/10.1164/rccm.200411-1586OC

Becker, S., & Soukup, J. M. (2003). Coarse (PM2.5-10), fine (PM2.5), and ultrafine air pollution particles induce/increase immune costimulatory receptors on human blood-derived monocytes but not on alveolar macrophages. *Journal of Toxicology and Environmental Health - Part A*, *66*(9), 847–859. https://doi.org/10.1080/15287390306381

Biswas, M. S., & Ayantika, D. C. (2021). Impact of covid-19 control measures on trace gases (NO_2, HCHO and SO_2) and aerosols over India during pre-monsoon of 2020. *Aerosol and Air Quality Research*, *21*(1), 1–20. https://doi.org/10.4209/aaqr.2020.06.0306

Bodor, Z., Bodor, K., Keresztesi, Á., & Szép, R. (2020). Major air pollutants seasonal variation analysis and long-range transport of PM10 in an urban environment with specific climate condition in Transylvania (Romania). *Environmental Science and Pollution Research*, *27*(30), 38181–38199. https://doi.org/10.1007/s11356-020-09838-2

Brown, S. G., Eberly, S., Paatero, P., & Norris, G. A. (2015). Methods for estimating uncertainty in PMF solutions: Examples with ambient air and water quality data and guidance on reporting PMF results. *Science of the Total Environment*, *518–519*, 626–635. https://doi.org/10.1016/j.scitotenv.2015.01.022

Chatterjee, A., Sarkar, C., Adak, A., Mukherjee, U., Ghosh, S. K., & Raha, S. (2013). Ambient air quality during diwali festival over Kolkata – A mega-city in ambient air quality during Diwali Festival over Kolkata – A mega-city in India. *Aerosol and Air Quality Research*, *13*(13), 1133. https://doi.org/10.4209/aaqr.2012.03.0062

Chen, L. H., Knutsen, S. F., Shavlik, D., Beeson, W. L., Petersen, F., Ghamsary, M., & Abbey, D. (2005). The association between fatal coronary heart disease and ambient particulate air pollution: Are females at greater risk? *Environmental Health Perspectives*, *113*(12), 1723–1729. https://doi.org/10.1289/ehp.8190

CPCB (2013). *Guidelines for the Measurement of Ambient Air Pollutants*. Central Pollution Control Board, 1, 11–30.

Deka, P., Bhuyan, P., Daimari, R., Sarma, K. P., & Hoque, R. R. (2016). Metallic species in PM10 and source apportionment using PCA-MLR modeling over mid-Brahmaputra Valley. *Arabian Journal of Geosciences*, *9*(5), 335. https://doi.org/10.1007/s12517-016-2368-z

Dimitriou, K., & Kassomenos, P. (2017). Airborne heavy metals in two cities of North Rhine Westphalia – Performing inhalation cancer risk assessment in terms of atmospheric circulation. *Chemosphere*, *186*, 78–87. https://doi.org/10.1016/j.chemosphere.2017.07.138

Diong, H. T., Das, R., Khezri, B., Srivastava, B., Wang, X., Sikdar, P. K., & Webster, R. D. (2016). Anthropogenic platinum group element (Pt, Pd, Rh) concentrations in PM10 and PM2.5 from Kolkata, India. *SpringerPlus*, *5*(1), 1242. https://doi.org/10.1186/s40064-016-2854-5

Dockery, D. W., Luttman-Gibson, H., Rich, D. Q., Link, M. S., Mittleman, M. A., Gold, D. R., Koutrakis, P., Schwartz, J. D., & Verrier, R. L. (2005). Association of air pollution with increased incidence of ventricular tachyarrhythmias recorded by implanted cardioverter defibrillators. *Environmental Health Perspectives*, *113*(6), 670–674. https://doi.org/10.1289/ehp.7767

Dutta, S., Ghosh, S., & Dinda, S. (2021). Urban air-quality assessment and inferring the association between different factors: A comparative study among Delhi, Kolkata and Chennai Megacity of India. *Aerosol Science and Engineering*, *5*(1), 93–111. https://doi.org/10.1007/s41810-020-00087-x

EzhilKumar, M. R., Karthikeyan, S., Chianese, E., Tirimberio, G., Di Gilio, A., Palmisani, J., Miniero, V. D., Cotugno, P., & Riccio, A. (2021). Vertical transport of PM2.5 and PM10 and its source identification in the street canyons of Chennai metropolitan city, India. *Atmospheric Pollution Research*, *12*(1), 173–183. https://doi.org/10.1016/j.apr.2020.08.032

Gajghate, D. G., Talwar, B., Pipalatkar, P., & Pustode, T. (2012). Chemical characterization of PM10 for metals in ambient air of Chennai, India. *Journal of Hazardous, Toxic, and Radioactive Waste*, *16*(2), 169–174. https://doi.org/10.1061/(asce)hz.1944-8376.0000079

Gajghate, D. G., Thawale, P. R., Vaidya, M.V., & Nema, P. (2005). Ambient respirable particulate matter and toxic metals in Kolkata City. *Bulletin of Environmental Contamination and Toxicology*, *75*(3), 608–614. https://doi.org/10.1007/s00128-005-0794-9

Gautam, S., & Hens, L. (2020). SARS-CoV-2 pandemic in India: What might we expect? *Environment, Development and Sustainability*, *22*(5), 3867–3869. https://doi.org/10.1007/s10668-020-00739-5

Ghermandi, G., Fabbi, S., Arvani, B., Veratti, G., Bigi, A., & Teggi, S. (2017). Impact assessment of pollutant emissions in the atmosphere from a power plant over a complex terrain and under unsteady winds. *Sustainability*, *9*(11), 2076. https://doi.org/10.3390/su9112076

Gogikar, P., Tyagi, B., Padhan, R. R., & Mahaling, M. (2018). Particulate matter assessment using in situ observations from 2009 to 2014 over an Industrial Region of Eastern India. *Earth Systems and Environment*, *2*(2), 305–322. https://doi.org/10.1007/s41748-018-0072-8

Gu, J., Pitz, M., Schnelle-Kreis, J., Diemer, J., Reller, A., Zimmermann, R., Soentgen, J., Stoelzel, M., Wichmann, H. E., Peters, A., & Cyrys, J.

(2011). Source apportionment of ambient particles: Comparison of positive matrix factorization analysis applied to particle size distribution and chemical composition data. *Atmospheric Environment*, *45*(10), 1849–1857. https://doi.org/10.1016/j.atmosenv.2011.01.009

Guo, H., Ding, A. J., So, K. L., Ayoko, G., Li, Y. S., & Hung, W. T. (2009). Receptor modeling of source apportionment of Hong Kong aerosols and the implication of urban and regional contribution. *Atmospheric Environment*, *43*(6), 1159–1169. https://doi.org/10.1016/j.atmosenv.2008.04.046

Gupta, A. K., Karar, K., & Srivastava, A. (2007). Chemical mass balance source apportionment of PM 10 and TSP in residential and industrial sites of an urban region of Kolkata, India. *Journal of Hazardous Materials*, *142*, 279–287. https://doi.org/10.1016/j.jhazmat.2006.08.013

Gupta, A. K., Karar, K., Ayoob, S., & John, K. (2008). Spatio-temporal characteristics of gaseous and particulate pollutants in an urban region of Kolkata, India. *Atmospheric Research*, *87*(2), 103–115. https://doi.org/10.1016/j.atmosres.2007.07.008

Gupta, A. K., Nag, S., & Mukhopadhyay, U. K. (2006). Characterisation of PM10, PM2.5 and benzene soluble organic fraction of particulate matter in an urban area of Kolkata, India. *Environmental Monitoring and Assessment*, *115*(1–3), 205–222. https://doi.org/10.1007/s10661-006-6550-8

Han, J. S., Moon, K. J., Lee, S. J., Kim, Y. J., Ryu, S. Y., Cliff, S. S., & Yi, S. M. (2006). Size-resolved source apportionment of ambient particles by positive matrix factorization at Gosan background site in East Asia. *Atmospheric Chemistry and Physics*, *6*(1), 211–223. https://doi.org/10.5194/acp-6-211-2006

Jain, S., Sharma, S. K., Choudhary, N., Masiwal, R., Saxena, M., Sharma, A., Mandal, T. K., Gupta, A., Gupta, N. C., & Sharma, C. (2017). Chemical characteristics and source apportionment of PM2.5 using PCA/APCS, UNMIX, and PMF at an urban site of Delhi, India. *Environmental Science and Pollution Research*, *24*(17), 14637–14656. https://doi.org/10.1007/s11356-017-8925-5

Jeričević, A., Gašparac, G., Mikulec, M. M., Kumar, P., & Prtenjak, M. T. (2019). Identification of diverse air pollution sources in a complex urban area of Croatia. *Journal of Environmental Management*, *243*, 67–77. https://doi.org/10.1016/j.jenvman.2019.04.024

Kabiraj, S., & Gavli, N. V. (2020). Impact of SARS-CoV-2 pandemic lockdown on air quality using satellite imagery with ground station monitoring data in most polluted city Kolkata, India. *Aerosol Science and Engineering*, *4*(4), 320–330. https://doi.org/10.1007/s41810-020-00077-z

Kar, S., Maity, J. P., Samal, A. C., & Santra, S. C. (2010). Metallic components of traffic-induced urban aerosol, their spatial variation, and source apportionment. *Environmental Monitoring and Assessment*, *168*(1–4), 561–574. https://doi.org/10.1007/s10661-009-1134-z

Karanasiou, A. A., Siskos, P. A., & Eleftheriadis, K. (2009). Assessment of source apportionment by Positive Matrix Factorization analysis on fine and coarse urban aerosol size fractions. *Atmospheric Environment*, *43*(21), 3385–3395. https://doi.org/10.1016/j.atmosenv.2009.03.051

Karar, K., Gupta, A. K., Kumar, A., & Biswas, A. K. (2006). Seasonal variations of PM10 and TSP in residential and industrial sites in an urban area of Kolkata, India. *Environmental Monitoring and Assessment*, *118*(1–3), 369–381. https://doi.org/10.1007/s10661-006-1503-9

Khobragade, P. P., & Ahirwar, A. V. (2019). Heavy metals in PM10 aerosols over an urban industrial city. *International Journal of Engineering and Advanced Technology*, *9*(1), 1402–1408. https://doi.org/10.35940/ijeat.a1225.109119

Kumar, A. V., Patil, R. S., & Nambi, K. S. V. (2001). Source apportionment of suspended particulate matter at two traffic junctions in Mumbai, India. *Atmospheric Environment*, *35*(25), 4245–4251. https://doi.org/10.1016/S1352-2310(01)00258-8

Larson, T., Gould, T., Simpson, C., Liu, L. J. S., Claiborn, C., & Lewtas, J. (2004). Source apportionment of indoor, outdoor, and personal $PM_{2.5}$ in Seattle, Washington, using positive matrix factorization. *Journal of the Air and Waste Management Association*, *54*(9), 1175–1187. https://doi.org/10.1080/10473289.2004.10470976

Liu, S., Krewski, D., Shi, Y., Chen, Y., & Burnett, R. T. (2003). Association between gaseous ambient air pollutants and adverse pregnancy outcomes in Vancouver, Canada. *Environmental Health Perspectives*, *111*(14), 1773–1778. https://doi.org/10.1289/ehp.6251

Liu, S., Zhou, Y., Liu, S., Chen, X., Zou, W., Zhao, D., Li, X., Pu, J., Huang, L., Chen, J., Li, B., Liu, S., & Ran, P. (2017). Association between exposure to ambient particulate matter and chronic obstructive pulmonary disease: Results from a cross-sectional study in China. *Thorax*, *72*(9), 788–795. https://doi.org/10.1136/thoraxjnl-2016-208910

Lodge, J. P. (1988). *Methods of Air Sampling and Analysis*. CRC Press, Taylor & Francis.

Mahato, S., Pal, S., & Ghosh, K. G. (2020). Effect of lockdown amid COVID-19 pandemic on air quality of the megacity Delhi, India. *Science of the Total Environment*, *730*, 139086. https://doi.org/10.1016/j.scitotenv.2020.139086

Majumdar, A., Satpathy, J., Kayee, J., & Das, R. (2020). Trace metal composition of rainwater and aerosol from Kolkata, a megacity in eastern India. *SN Applied Sciences*, *2*(12), 1–17. https://doi.org/10.1007/s42452-020-03933-2

Moreno, T., Querol, X., Alastuey, A., García Do Santos, S., Fernández Patier, R., Artiñano, B., & Gibbons, W. (2006). PM source apportionment and trace metallic aerosol affinities during atmospheric pollution episodes: A case study from Puertollano, Spain. *Journal of Environmental Monitoring*, *8*(10), 1060–1068. https://doi.org/10.1039/b608321h

Mousavi, A., Sowlat, M. H., & Sioutas, C. (2018). Diurnal and seasonal trends and source apportionment of redox-active metals in Los Angeles using a novel online metal monitor and Positive Matrix Factorization (PMF). *Atmospheric Environment*, *174*, 15–24. https://doi.org/10.1016/j.atmosenv.2017.11.034

Muhammad, S., Long, X., & Salman, M. (2020). COVID-19 pandemic and environmental pollution: A blessing in disguise? *Science of the Total Environment*, *728*, 138820. https://doi.org/10.1016/j.scitotenv.2020.138820

Nath, B., Majumder, S., Sen, J., & Rahman, M. M. (2021). Risk analysis of COVID-19 infections in Kolkata Metropolitan city: A GIS-based study and policy implications. *GeoHealth*, *5*(4), 1–17. https://doi.org/10.1029/2020GH000368

Pandis, N. (2016). Two-way analysis of variance: Part 2. *American Journal of Orthodontics and Dentofacial Orthopedics*, *149*(1), 137–139. https://doi.org/10.1016/j.ajodo.2015.10.007

Parvizimehr, A., Baghani, A. N., Hoseini, M., Sorooshian, A., Cuevas-Robles, A., Fararouei, M., Dehghani, M., Delikhoon, M., Barkhordari, A., Shahsavani, S., & Badeenezhad, A. (2020). On the nature of heavy metals in PM_{10} for an urban desert city in the Middle East: Shiraz, Iran. *Microchemical Journal*, *154*, 104596. https://doi.org/10.1016/j.microc.2020.104596

Prabakaran, P., & Manikandan, A. (2018). Present tendency of inorganic metal traces in the atmosphere of Chennai City. *International Journal of Mechanical Engineering and Technology*, *9*(7), 1231–1239.

Prati, P., Zucchiatti, A., Lucarelli, F., & Mandò, P. A. (2000). Source apportionment near a steel plant in Genoa (Italy) by continuous aerosol sampling and PIXE analysis. *Atmospheric Environment*, *34*(19), 3149–3157. https://doi.org/10.1016/S1352-2310(99)00421-5

Rajput, P., Mandaria, A., Kachawa, L., Singh, D. K., Singh, A. K., & Gupta, T. (2016). Chemical characterisation and source apportionment of PM1 during massive loading at an urban location in Indo-Gangetic Plain: Impact of local sources and long-range transport. *Tellus, Series B: Chemical and Physical Meteorology*, *68*(1), 30659. https://doi.org/10.3402/tellusb.v68.30659

Reff, A., Eberly, S. I., & Bhave, P. V. (2007). Receptor modeling of ambient particulate matter data using positive matrix factorization: Review of existing methods. *Journal of the Air & Waste Management Association*, *57*(2), 146–154. https://doi.org/10.1080/10473289.2007.10465319

Sangani, R. G., Soukup, J. M., & Ghio, A. J. (2010). Metals in air pollution particles decrease whole-blood coagulation time. *Inhalation Toxicology*, *22*(8), 621–626. https://doi.org/10.3109/08958371003599037

Sarkar, M., Das, A., & Mukhopadhyay, S. (2021). Assessing the immediate impact of COVID-19 lockdown on the air quality of Kolkata and Howrah, West Bengal, India. *Environment, Development and Sustainability*, *23*(6), 8613–8642. https://doi.org/10.1007/s10668-020-00985-7

Shi, G. L., Zeng, F., Li, X., Feng, Y. C., Wang, Y. Q., Liu, G. X., & Zhu, T. (2011). Estimated contributions and uncertainties of PCA/MLR-CMB results: Source apportionment for synthetic and ambient datasets. *Atmospheric Environment*, *45*(17), 2811–2819. https://doi.org/10.1016/j.atmosenv.2011.03.007

Singh, V., Singh, S., Biswal, A., Kesarkar, A. P., Mor, S., & Ravindra, K. (2020). Diurnal and temporal changes in air pollution during COVID-19 strict lockdown over different regions of India. *Environmental Pollution*, *266*, 115368. https://doi.org/10.1016/j.envpol.2020.115368

Srivastava, D., Goel, A., & Agrawal, M. (2016). Particle bound metals at major intersections in an urban location and source identification through use of metal markers. *Proceedings of the National Academy of Sciences India Section A - Physical Sciences*, *86*(2), 209–220. https://doi.org/10.1007/s40010-016-0268-y

Srivastava, S., Kumar, A., Bauddh, K., Gautam, A. S., & Kumar, S. (2020). 21-day lockdown in india dramatically reduced air pollution indices in Lucknow and New Delhi, India. *Bulletin of Environmental Contamination and Toxicology*, *105*(1), 9–17. https://doi.org/10.1007/s00128-020-02895-w

Villanueva, F., Ródenas, M., Ruus, A., Saffell, J., & Gabriel, M. F. (2021). Sampling and analysis techniques for inorganic air pollutants in indoor air. *Applied Spectroscopy Reviews*, *0*(0), 1–49. https://doi.org/10.1080/05704928.2021.2020807

Wu, J., Li, J., Teng, Y., Chen, H., & Wang, Y. (2020). A partition computing-based positive matrix factorization (PC-PMF) approach for the source apportionment of agricultural soil heavy metal contents and associated health risks. *Journal of Hazardous Materials*, *388*, 121766. https://doi.org/10.1016/j.jhazmat.2019.121766

Wu, Y., Lu, B., Zhu, X., Wang, A., Yang, M., Gu, S., Wang, X., Leng, P., Zierold, K. M., Li, X., Tang, K. K., Fang, L., Huang, R., Xu, G., & Chen, L. (2019). Seasonal variations, source apportionment, and health risk assessment of heavy metals in $PM_{2.5}$ in Ningbo, China. *Aerosol and Air Quality Research*, *19*(9), 2083–2092. https://doi.org/10.4209/aaqr.2018.12.0452

Yu, L., Wang, G., Zhang, R., Zhang, L., Song, Y., Wu, B., Li, X., An, K., & Chu, J. (2013). Characterization and source apportionment of PM2.5 in an urban environment in Beijing. *Aerosol and Air Quality Research*, *13*(2), 574–583. https://doi.org/10.4209/aaqr.2012.07.0192

Zalakeviciute, R., Rybarczyk, Y., Granda-Albuja, M. G., Diaz Suarez, M. V., & Alexandrino, K. (2020). Chemical characterization of urban PM10 in the Tropical Andes. *Atmospheric Pollution Research*, *11*(2), 343–356. https://doi.org/10.1016/j.apr.2019.11.007

SUPPORTING INFORMATION

Additional supporting information may be found in the online version of the article at the publisher's website.

How to cite this article: Tudu, P., Gaine, T., Mahanty, S., Mitra, S., Bhattacharyya, S., & Chaudhuri, P. (2022). Impact of COVID-19 lockdown on the elemental profile of PM_{10} present in the ambient aerosol of an educational institute in Kolkata, India. *Environ Qual Manage.* 1–18. https://doi.org/10.1002/tqem.21862